Tight-Binding Approach to Electrons in a Crystal Potential and an External Magnetic Field

E. GERLACH AND D. LANGBEIN
Battelle-Institut, Frankfurt-am-Main, Germany
(Received 1 February 1965; revised manuscript received 8 November 1965)

A general transformation of the tight-binding determinant for a finite orthorhombic crystal in an external magnetic field is introduced. It yields interacting finite Peierls determinants, where the interaction terms arise from distinct surfaces. This result is applied to the energy structure of wires and foils. The formation of Landau levels is demonstrated. The gap widths obtained in films are applicable also to infinite crystals. It is shown that the level broadening near the edges of the unperturbed band and the gap widths near the center decrease exponentially with the magnetic field.

I. INTRODUCTION

In view of the increasing importance attached to magnetic and galvanomagnetic effects much attention has been given to the eigenstates of electrons in a crystal potential in the presence of a magnetic field B. Until now this problem has been treated only for infinite crystals, using either a high-field approach,[1,2] or the $E(\hat{k})$ operator[3–11] introduced by Peierls, or general symmetry considerations.[1,11,12] These methods furnish the well-known Landau levels at the energy band edges, which are broadened according to the relative positions of the magnetic vector potential and the lattice. Broadening increases as the distance of the levels increases from the band edges.

It is the objective of the present work to investigate the energy structure of finite crystals. We use a one-band tight-binding approximation; our procedure, therefore, has several analogies to the Peierls' treatment.[3] Peierls shows that the Hamiltonian for infinite crystals can be replaced by the operator $E(\hat{k})$ where $E(k)$ is the electron energy for vanishing magnetic field and $\hat{k}$ obeys the commutation relation $[\hat{k},\hat{k}]=iB$. Consideration of the translational properties of $E(\hat{k})$ yields a difference equation for the eigenfunctions and a secular determinant for the corresponding energies. For an orthorhombic lattice this determinant is three-diagonal, in the following this will be referred to as Peierls' determinant.

Since in a finite lattice the wave vector k has only discrete values, it is difficult in this case to establish a correspondence between k and $\hat{k}$. Instead, we start directly from the Hamiltonian of a finite orthorhombic lattice (Sec. IIA) and construct auxiliary functions so that the matrix elements of the Hamiltonian between the latter and all atomic orbitals vanish except those at one surface (Sec. IIB). A variational treatment then yields a secular determinant, which has the order N_2 (Sec. IIC) and whose elements in the principal diagonal are finite Peierls' determinants of the order N_1 (Sec. IID). N_1, N_2 are the numbers of unit cells in the directions normal to the magnetic field. The remaining elements of this secular determinant originate from surfaces. They vanish with vanishing magnetic field and increasing N_2 (Sec. IIE).

In Sec. III the results obtained in Sec. II are applied to wires and films. The surface terms yield a linear or quadratic repulsion of degenerate levels in wires according to the symmetry properties of the wave functions (Sec. IIIA). The energy structure of films is represented by the principal diagonal elements, which are handled by a second-order perturbation treatment. We obtain a repulsion of the unperturbed energy levels at the band edges and a concentration in the center of the band, which indicates the manner of formation of Landau levels in infinite crystals (Sec. IIIB). The width of the adjoined energy gaps is determined in a high-field approach in Sec. IIIC. A rigorous investigation of the energy structure, carried out for infinite crystals and special values of the magnetic flux in Sec. IIID, verifies the results obtained before and visualizes the transition to weak fields.

II. A GENERAL FORMALISM FOR FINITE CRYSTALS

A. Tight-Binding Matrix Elements

For an electron in a finite periodic crystal potential $G(r)$ and in a homogeneous magnetic field B described by the vector potential $A(r)=\frac{1}{2}[B,r]$ we have the Schrödinger equation

$$H|E\rangle=\{\tfrac{1}{2}(-i\nabla+A(r))^2+G(r)\}|E\rangle=E|E\rangle. \quad (1)$$

For simplicity, we consider an orthorhombic crystal with the basis vectors a_i ($i=1, 2, 3$) and magnetic fields B parallel to a_3. Let the number of atoms in these three directions be N_1, N_2, N_3. $|n\rangle$ denotes the normalized electron orbital of an isolated atom at the position $n=\sum_i n_i a_i$ ($n_i=1, 2, \cdots, N_i$), the orbital being equal

[1] J. Zak, Phys. Rev. **136**, A776 (1964).
[2] A. Jannussis, Phys. Status Solidi **6**, 217 (1964).
[3] R. Peierls, Z. Physik **80**, 763 (1933).
[4] W. Kohn and J. M. Luttinger, Phys. Rev. **97**, 869 (1955).
[5] G. E. Zilbermann, Zh. Eksperim. i Teor Fiz. **30**, 1092 (1956) [English transl.: Soviet Phys.—JETP **3**, 835 (1957)].
[6] W. Kohn, Phys. Rev. **115**, 1460 (1959).
[7] R. G. Chambers, Can. J. Phys. **34**, 1395 (1956).
[8] E. J. Blount, Phys. Rev. **126**, 1636 (1962).
[9] L. M. Roth, J. Phys. Chem. Solids **23**, 433 (1962).
[10] J. Schnakenberg, Z. Physik **171**, 199 (1963).
[11] E. Brown, Phys. Rev. **133**, A1038 (1964).
[12] H. J. Fischbeck, Phys. Status Solidi **3**, 1082 (1963).

gauged[3] by multiplication with the factor $\exp[-irA(n)]$. In order to separate the Hamiltonian with respect to the direction of the field we use the following expression

$$|n_1n_2\theta_3\rangle=(2/(N_3+1))^{1/2}\sum_{n_3=1}^{N_3}\sin n_3\theta_3|n\rangle. \quad (2)$$

The sine factor corresponds to the tight-binding wave function of an electron in a finite crystal[13] without magnetic field. The boundary conditions for $|n_1n_2\theta_3\rangle$ in the a_3 direction are satisfied if θ_3 takes the values $\mu_3\pi/(N_3+1)$, $(\mu_3=1,\cdots,N_3)$. Forming matrix elements of $H-E$ with $|n_1n_2\theta_3\rangle$, we obtain

$$\langle n_1'n_2'\theta_3'|H-E|n_1n_2\theta_3\rangle=(2/(N_3+1))\sum_{n_3',n_3}\sin n_3'\theta_3'\times\sin n_3\theta_3 e^{inA(n')}\langle n'-n|H-E|0\rangle. \quad (3)$$

In (3) the gauging relation

$$\langle n'|H-E|n\rangle=\langle n'-n|H-E|0\rangle e^{inA(n')} \quad (4)$$

is utilized; ket $|0\rangle$ is introduced for simplicity.

When using a nearest-neighbor approximation only those matrix elements are different from zero for which $n_i'=n_i$, $n_i\pm1$; $n_j'=n_j$ $(i\neq j)$. Taking (4) into account, we define the following abbreviations

$$\begin{aligned}&H=\langle0|H-E|0\rangle,\\&K_1=\langle1\,0\,0|H-E|0\rangle=\langle-1\,0\,0|H-E|0\rangle^*,\\&K_2=\langle0\,1\,0|H-E|0\rangle=\langle0\,-1\,0|H-E|0\rangle^*,\\&K_3=\langle0\,0\,1|H-E|0\rangle=\langle0\,0\,-1|H-E|0\rangle.\end{aligned} \quad (5)$$

K_1, K_2, and K_3 are interaction integrals, which depend to a minor extent on the magnetic field. For simplicity this B dependence is neglected in the following. By inserting (5) we obtain from (3)

$$\begin{aligned}&\langle n_1'n_2'\theta_3'|H-E|n_1n_2\theta_3\rangle\\&=\delta(\theta_3',\theta_3)e^{inA(n')}\{(H_0+2K_3\cos\theta_3)\delta(n_1',n_1)\delta(n_2',n_2)\\&\quad+(K_1\delta(n_1',n_1+1)+K_1^*\delta(n_1',n_1-1))\delta(n_2',n_2)\\&\quad+(K_2\delta(n_2',n_2+1)+K_2^*\delta(n_2',n_2-1))\delta(n_1',n_1)\}.\end{aligned} \quad (6)$$

The δ function arises from the orthogonality relation

$$(2/(N_i+1))\textstyle\sum_{n_i}\sin n_i\theta_i'\sin n_i\theta_i=\delta(\theta_i',\theta_i), \quad (7)$$

for

$$\theta_i',\ \theta_i=\mu_i\pi/(N_i+1);\quad \mu_i=1,\cdots,N_i;\quad i=1,2,3.$$

B. Construction of an Auxiliary Function by a Diagram Technique

In the tight-binding method the solution of the Schrödinger equation is expressed as a linear combination of the orbitals. Thus, the secular determinant following from a variational treatment has to be built up from the matrix elements (6).

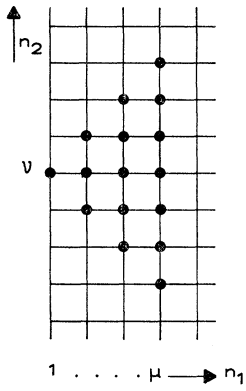

FIG. 1. Wave functions contained in the auxiliary function $|\mu\nu\theta_3\rangle$.

In order to reduce this determinant and to give it a form which is related to that obtained from the Peierls $E(\hat{k})$ operator[14,15] for infinite crystals, we now introduce an appropriate auxiliary function $|\mu\nu\theta_3\rangle$. For the moment we consider a semi-infinite lattice with $1\leq n_1\leq+\infty$, $-\infty\leq n_2\leq+\infty$ and construct $|\mu\nu\theta_3\rangle$ as a linear combination of those wave functions $|n_1n_2\theta_3\rangle$, which are located within the triangle shown in Fig. 1. ν denotes the position and μ the extension of this triangle. We define

$$|\mu\nu\theta_3\rangle=\sum_{n_1=1}^{\mu}\sum_{n_2=\nu-n_1+1}^{\nu+n_1-1}u_\nu(n_1,n_2)|n_1n_2\theta_3\rangle \quad (8)$$

$$(1\leq\mu\leq+\infty,\ -\infty\leq\nu\leq+\infty)$$

with $u_\nu(1,\nu)=1$ and determine the coefficients $u_\nu(n_1,n_2)$, $n_1>1$ from the condition

$$\langle n_1'n_2'\theta_3|H-E|\mu\nu\theta_3\rangle=0 \quad (9)$$

for $n_1'<\mu$, n_2' arbitrary.

This means that the matrix elements of $H-E$ between the auxiliary functions and the original wave functions are claimed to vanish for all wave functions except for those on the plane $n_1=\mu$. According to the particular properties of $|\mu\nu\theta_3\rangle$ the insertion of (8) into (9) yields

$$\begin{aligned}&\langle n_1n_2\theta_3|H-E|n_1\nu\theta_3\rangle\\&\quad+u_\nu(n_1+1,n_2)\langle n_1n_2\theta_3|H-E|n_1+1,n_2\theta_3\rangle=0.\end{aligned} \quad (10)$$

From a further evaluation of (10) we obtain a recurrence formula for $u_\nu(n_1,n_2)$

$$\begin{aligned}&[H_0+2K_3\cos\theta_3-E]u_\nu(n_1,n_2)+K_1e^{i(b/2)n_2}u_\nu(n_1-1,n_2)\\&\quad+K_1^*e^{-i(b/2)n_2}u_\nu(n_1+1,n_2)+K_2e^{-i(b/2)n_1}u_\nu(n_1,n_2-1)\\&\quad+K_2^*e^{i(b/2)n_1}u_\nu(n_1,n_2+1)=0\end{aligned} \quad (11)$$

with

$$\begin{aligned}&u_\nu(n_1,n_2)=0\quad\text{for}\quad|n_2-\nu|\geq n_1;\\&u_\nu(1,n_2)=\delta(n_2-\nu,0).\end{aligned} \quad (12)$$

b denotes the magnetic flux ($B[a_1,a_2]$) through the unit cell. Since the boundary condition (12) depends only

[13] T. B. Grimley, J. Phys. Chem. Solids **14**, 227 (1960).

[14] P. G. Harper, Proc. Phys. Soc. (London) **A68**, 874 (1955).

[15] A. D. Brailsford, Proc. Phys. Soc. (London) **A70**, 275 (1957).

on $n_2-\nu$, we find that $u_\nu(n_1,n_2)$,except for a factor $\exp[ib\nu(n_1-1)/2]$, is also a function of $n_2-\nu$. Writing $K_j=|K_j|e^{i\alpha j}$, $(j=1, 2)$, we represent $u_\nu(n_1,n_2)$ by

$$u_\nu(n_1,n_2)=e^{i(b/2)\nu(n_1-1)} \times e^{i[\alpha_1(n_1-1)+\alpha_2(n_2-\nu)]}v(n_1-1, n_2-\nu) \quad (13)$$

and obtain for $v(n_1,n_2)$ the simplified recurrence equation

$$\begin{aligned} H_0'V(n_1,n_2)&+|K_1|e^{i(b/2)n_2}v(n_1-1, n_2) \\ &+|K_1|e^{-i(b/2)n_2}v(n_1+1, n_2) \\ &+|K_2|e^{-i(b/2)n_1}v(n_1, n_2-1) \\ &+|K_2|e^{i(b/2)n_1}v(n_1, n_2+1)=0 \end{aligned} \quad (14)$$

and the boundary condition

$$v(n_1,n_2)=0 \quad \text{for} \quad |n_2|>n_1; \quad v(0,n_2)=\delta(0,n_2). \quad (15)$$

H_0' is an abbreviation for $H_0+2K_3\cos\theta_3-E$.

For evaluating $v(n_1,n_2)$ it is convenient to introduce a diagram technique. According to (14), contributions to $v(n_1+1, n_2)$ arise only from $v(n_1,n_2)$, $v(n_1, n_2\pm1)$, and $v(n_1-1, n_2)$. This can be represented by diagrams between the corresponding lattice points, as shown in Fig. 2.

The factors adjoined to the diagrams in Fig. 2 are taken from (14). n_1 and n_2 refer to the positions designated by the dot at the origins of the diagrams.

$v(n_1,n_2)$ is now obtained by drawing all arrangements of the above diagrams connecting the points (0,0) and (n_1,n_2) and by summing the adjoined products over these paths.

As an example we calculate $v(2,0)$. Figure 3 shows the four possible paths and the products adjoined. The sum over the paths yields

$$v(2,0)=(H_0'^2+2|K_2|^2\cos b-|K_1|^2)/|K_1|^2. \quad (16)$$

The path resulting from the inversion of an arbitrary allowed path from (0,0) to (n_1,n_2) at the point $(\frac{1}{2}n_1, \frac{1}{2}n_2)$ is also allowed. The diagram technique adjoins to it the same interaction integrals and, on the other hand, the complex conjugate of the exponential factor; thus $v(n_1,n_2)$ is necessarily real. Reflection of an allowed path from (0,0) to (n_1,n_2) at $n_2=0$, on the other hand,

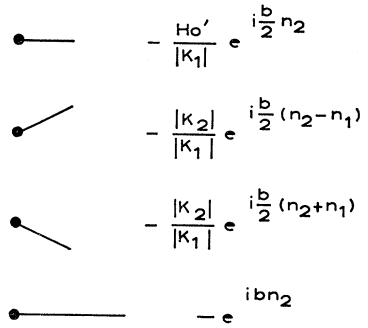

FIG. 2. Allowed diagrams and adjoined factors.

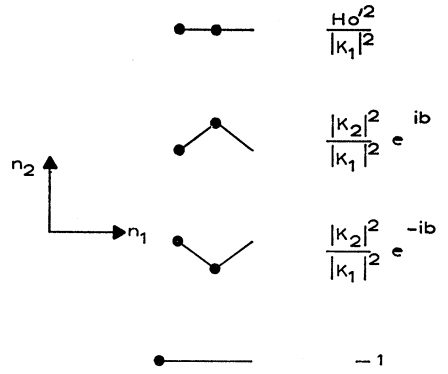

FIG. 3. Paths of diagrams contributing to $v(2,0)$.

yields an allowed path from (0,0) to $(n_1, -n_2)$. We again have to adjoin the same interaction integrals and the complex-conjugate exponential. Therefore, we conclude

$$v(n_1,n_2)=v^*(n_1, -n_2)=v(n_1, -n_2). \quad (17)$$

C. Variational Treatment of Finite Crystals

We now perform a variational treatment for the finite crystal of Sec. IIA. We utilize the fact that the matrix elements of $H-E$ between the auxiliary functions $|N_1\nu\theta_3)$, $\nu=1, \cdots, N_2$, which in the a_1 direction have the same extension as the crystal, and the wave functions $|n_1n_2\theta_3\rangle$ vanish except for those at the surface. In order to exclude wave functions from outside the finite crystal (to be consistent with the tight-binding approximation employed), we also change the auxiliary functions which overlap the boundaries $n_2=1$, N_2, so that only wave functions of the finite crystal are involved. Then, instead of (9), we claim that those matrix elements vanish which are formed by the wave functions of the crystal under consideration. This results in a change of $u_\nu(n_1,n_2)$ with ν near the boundaries $n_2=1$, N_2. We introduce a generalized function $v(n_1,n_2,\nu)$, which can be obtained from the diagram method by drawing all paths from $(0,\nu)$ to (n_1,n_2), using $\tilde{n}_2=n_2-\nu$ for calculating the adjoined products and leaving out all paths which cross the boundaries. $V(n_1,n_2,\nu)$ thus is equal to $v(n_1, n_2, -\nu)$ for $\nu+n_2$, $2(N_2+1)-\nu-n_2>n_1$ and modified for $\nu+n_2$, $2(N_2+1)-\nu-n_2\leq n_1$.

The variational treatment yields a secular determinant closely related to those derived from the Peierls treatment, if we transform the wave functions according to

$$|N_1\theta_2\theta_3)=(2/(N_2+1))^{1/2}e^{i\alpha_1(N_1-1)} \times\textstyle\sum_\nu e^{-i[(b/2)N_1-\alpha_2]\nu}\sin\nu\theta_2|N_1\nu\theta_3) \quad (18)$$

and

$$|N_1\theta_2\theta_3\rangle=(2/(N_2+1))^{1/2} \times\textstyle\sum_{n_2} e^{-i[(b/2)-\alpha_2]n_2}\sin n_2\theta_2|N_1n_2\theta_3\rangle, \quad (19)$$

$\theta_2=\mu_2\pi/(N_2+1)$, $\mu_2=1, \cdots, N_2$. Using (10), (13), (18),

and (19) the matrix element is found to be

$$\langle N_1\theta_2'\theta_3|H-E|N_1\theta_2\theta_3\rangle$$
$$=-|K_1|\frac{2}{N_2+1}\sum_{n_2,\nu=1}^{N_2}\sin n_2\theta_2'\sin\nu\theta_2 v(N_1,n_2,\nu). \quad (20)$$

In (20) the sum over n_2 can be extended to $-\infty\leq n_2\leq+\infty$ if we maintain that paths crossing the boundaries are disregarded in the calculation of $v(N_1,n_2,\nu)$. Using again $\tilde{n}_2=n_2-\nu$ and taking (17) into account we obtain

$$\langle||\rangle=\sum_{\tilde{n}_2=-N_1}^{+N_1}v(N_1,\tilde{n}_2)\cos\tilde{n}_2\theta_2\,\delta(\theta_2',\theta_2)$$
$$-\frac{2}{N_2+1}\sum_{n_2=-\infty}^{+\infty}\sum_{\nu=1}^{N_2}\sin n_2\theta_2'\sin\nu\theta_2\sum_j g_j(n_2,\nu), \quad (21)$$

where the first term originates from extending $v(N_1,n_2,\nu)$ to $v(N_1,n_2-\nu)$. In the second term the excess paths of the first are compensated, i.e., j runs over all paths from $(0,\nu)$ to (N_1,n_2) which cross the boundary and $g_j(n_2,\nu)$ designates the adjoined products. It is noted that, owing to the δ function in the first term, the bulk of the crystal and the surfaces $n_1=1$, N_1 influence only the principal diagonal of the secular determinant, whereas the other elements arise from the surfaces $n_2=1$, N_2. For convenience the first term will be called bulk term.

D. The Bulk Term

For further evaluation of the first term of (21) we note that it is a polynomial of the order N_1 with respect to the energy E; we call it $P(N_1,\theta_2)$. Using the recurrence formula (14) for $v(n_1,n_2)$ and the symmetry relation (17) we obtain a recurrence equation for $P(N_1,\theta_2)$:

$$|K_1|\{P(N_1+1,\theta_2)$$
$$+\tfrac{1}{2}[P(N_1-1,\theta_2+b)+P(N_1-1,\theta_2-b)]\}$$
$$=\tfrac{1}{2}\{[H_0'+2|K_2|\cos(\theta_2-\tfrac{1}{2}N_1b)]P(N_1,\theta_2+\tfrac{1}{2}b)$$
$$+[H_0'+2|K_2|\cos(\theta_2+\tfrac{1}{2}N_1b)]P(N_1,\theta_2-\tfrac{1}{2}b)\}. \quad (22)$$

For the initial values we have

$$P(0,\theta_2)=1;\quad P(1,\theta_2)=(H_0'+2|K_2|\cos\theta_2)/|K_1|. \quad (23)$$

From (22), (23) we find the following representation for $P(N_1,\theta_2)$:

$$|K_1|^{N_1}P(N_1,\theta_2)=\det p_{\kappa',\kappa}$$
$$p_{\kappa',\kappa}=H_0'+2|K_2|\cos\left[\theta_L-\frac{1}{L}(N_1-2\kappa+1)b\right],\quad \kappa'=\kappa$$
$$=|K_1|,\quad \kappa'=\kappa\pm1 \quad (24)$$
$$=0,\qquad \text{otherwise};$$
$$\kappa',\kappa=1,\cdots,N_1.$$

For the proof of (24) we note that it satisfies the recurrence equations

$$|K_1|[P(N_1+1,\theta_2)+P(N_1-1,\theta_2\pm b)]$$
$$=[H_0'+2|K_2|\cos(\theta_2\mp\tfrac{1}{2}N_1b)]P(N_1,\theta_2\pm\tfrac{1}{2}b) \quad (25)$$

and the initial condition (23). Addition of the two recurrence equations (25) yields (22).

Equation (24) can be interpreted as being a part of an infinite Peierls' determinant for an orthorhombic lattice. The fact that the order of the determinant is N_1 arises from the special choice of our auxiliary functions. By rotation of these auxiliary functions by $\frac{1}{2}\pi$ around the field direction, N_1, θ_2 could be changed into N_2,θ_1. Our choice is reasonable for a crystal with $N_1\leq N_2$; thus the surface terms in (21) are expected to be less important than the bulk terms.

For foils the surface terms will vanish perfectly, and we are left only with (24). This case will be discussed in Sec. III.

E. The Surface Terms

We now investigate the second term of (21), which contains all paths crossing the surfaces. Paths which cross both of the boundaries $n_2=1$, N_2 are excluded by assuming $N_1\leq N_2+2$. In this case the sum over n_2 and ν is split into partial sums with respect to the two boundaries. In addition, we distinguish the cases where n_2 denotes positions inside or outside the crystal. From (21) we obtain

$$\langle||\rangle_{\text{surf}}=-\frac{2}{N_2+1}\{\sum_{\nu=1}^{N_1-1}(\sum_{n_2=\nu-N_1}^{-1}+\sum_{n_2=1}^{N_1-\nu})$$
$$+\sum_{\nu=N_2+2-N_1}^{N_2}(\sum_{n_2=2(N_2+1)-N_1-\nu}^{N_2}+\sum_{n_2=N_2+2}^{N_1+\nu})\}$$
$$\times\sin n_2\theta_2'\sin\nu\theta_2\sum_j g_j(n_2,\nu). \quad (26)$$

Now, we introduce a one-to-one correspondence between the paths starting and ending inside the crystal and those starting inside and ending outside. Let a path j starting and ending inside meet the lines $n_2=0$ or $n_2=N_2+1$ for the first time at $n_1=n_{1c}$. Let the corresponding path j from the inside to the outside be that which is the same for $n_1\leq n_{1c}$ and folded around $n_2=0$ or $n_2=N_2+1$ for $n_1\geq n_{1c}$. From the diagram technique we conclude that the adjoined products of the two paths are identical with respect to the interaction integrals and differ in the exponentials. Changing n_2 into $-n_2$ or $2(N_2+1)-n_2$ in those sums of (26) which run over positions inside the crystal, and utilizing the fact that $\sin n_2\theta_2$ is odd with respect to $n_2=0$, N_2+1, we obtain

$$\langle||\rangle_{\text{surf}}=-(2/(N_2+1))\{\sum_{\nu=1}^{N_1-1}\sum_{n_2=\nu-N_1}^{-1}+\sum_{\nu=N_2+2-N_1}^{N_2}\sum_{n_2=N_2+2}^{N_1+\nu}\}$$
$$\times\sin n_2\theta_2'\sin\nu\theta_2\sum_j[g_j(n_2,\nu)-g_j(-n_2,\nu)]. \quad (27)$$

As a result of the introduced correspondence of paths, the bracket in (27) is proportional to the magnetic flux b. A further simplification of (27) is achieved by taking into account that a reflection of a path at a line $n_2=$const generates the complex-conjugate adjoined product. Thus, by reflection of the paths crossing the upper boundary $n_2=N_2$, we obtain

$$\langle|\,|\rangle_{\text{surf}}=-(2/(N_2+1))\sum_{\nu=1}^{N_1-1}\sum_{n_2=\nu-N_1}^{-1}\sin n_2\theta_2'\sin\nu\theta_2$$
$$\times\sum_j\{[g_j(n_2,\nu)-g_j(-n_2,\nu)]$$
$$+(-1)^{\mu_2'+\mu_2}[g_j^*(n_2,\nu)-g_j^*(-n_2,\nu)]\}, \quad (28)$$

where we used the relation $\theta_2=\mu_2\pi/(N_2+1)$.

We note the following properties of (28): Since the number of terms to be summed depends merely on N_1, the matrix element is proportional to $1/(N_2+1)$. If θ_2' or θ_2 take small values, which corresponds to the energy band edges for vanishing magnetic field, $\langle|\,|\rangle_{\text{surf}}$ becomes small also. The brace in (28) is proportional to b for $\mu_2'+\mu_2$ odd and to b^2 for $\mu_2'+\mu_2$ even. This is due to the fact that the terms in each bracket differ merely in their exponentials as described above. The properties of $\langle|\,|\rangle_{\text{surf}}$ will reappear in the repulsion of the energy levels of wires.

III. APPLICATION TO WIRES, FILMS AND INFINITE CRYSTALS

A. Energy Levels of Wires

The general formalism developed in Sec. II furnished a secular determinant of the order N_2 whose principal diagonal elements consist, essentially, of finite Peierls' determinants of the order N_1. Now, this result is applied to the energy levels of electrons in wires in the a_3 direction. Wires parallel to a_1 or a_2 are discussed in connection with films below. As is seen from (24) each bulk term $P(N_1,\theta_2)$ is a quadratic function of b. Since its eigenvalues are not degenerate for vanishing fields, the level splitting arising from $P(N_1,\theta_2)$ is also quadratic in b. We will show that the surface terms, on the other hand, yield a linear splitting; thus they are more important in the case of small fields under consideration.

Degenerate levels for vanishing field belong to different principal diagonal elements of the secular determinant. In order to determine the splitting originating from the surface terms, we apply the common perturbation treatment for degenerate levels and are left with a subdeterminant of the order of the degeneracy. For a twofold degeneracy belonging to $P(N_1,\theta_2')$ and $P(N_1,\theta_2)$ the level splitting is represented by the surface term (28) divided by an energy denominator, which describes an average distance from the remaining levels of $P(N_1,\theta_2')$ and $P(N_1,\theta_2)$. From Sec. IIE we have the result that splitting is proportional to b for $\mu_2'+\mu_2$ odd or to b^2 for $\mu_2'+\mu_2$ even, which corresponds to the symmetry properties of the wave functions. For $\mu_2'+\mu_2$ odd, one of the wave functions is even, the other one odd with respect to a reflection at $n_2=\frac{1}{2}N_2$; for $\mu_2'+\mu_2$ even, both of the two wave functions are even or both are odd. The dependence of the splitting on the crystal dimension in the a_2 direction is given by $1/(N_2+1)$. Also, the splitting is small at the band edges corresponding to the a_2 direction and large at the band edges corresponding to the a_1 direction.

In order to visualize the above results, we investigate those contributions in (28) which arise from paths with $\nu-n_2=N_1$, N_1-1 and therefore describe (28) completely up to $N_1=3$, and plot the level scheme for a wire with $N_1=N_2=3$. For $\nu-n_2=N_1$ there is only one path from $(0,\nu)$ to (N_1,n_2); we obtain the adjoined product $g(n_2,\nu)=(-|K_2/K_1|)^{N_1}$ and by folding $g(-n_2,\nu)=(-|K_2/K_1|)^{N_1}\exp(ib\nu n_2/2)$. For $\nu-n_2=N_1-1$ we find N_1 possible paths. Summing over j and expanding for small b we obtain from (28)

$$\langle|\,|\rangle_{\text{surf}}=\left(-\frac{|K_2|}{|K_1|}\right)^{N_1}\frac{2}{N_2+1}$$
$$\times\Big[\sum_{\nu=1}^{N_1-1}\sin\nu\theta_2\sin(N_1-\nu)\theta_2'\gamma_1(\nu)+\frac{H_0'}{|K_2|}$$
$$\times\sum_{\nu=1}^{N_1-2}\sin\nu\theta_2\sin(N_1-\nu-1)\theta_2'\gamma_2(\nu)+\cdots\Big],$$
$$\gamma_1(\nu)=b^2\nu^2(N_1-\nu)^2$$
$$=2ib\nu(N_1-\nu),$$
$$\gamma_2(\nu)=b^2\nu(N_1-\nu-1)[(N_1+2)\nu(N_1-\nu-1)-1]$$
$$=2ib\nu(N_1-\nu-1)(N_1+1), \quad (29)$$

where the upper expressions are valid for $\mu_2'+\mu_2$ even, the lower ones for $\mu_2'+\mu_2$ odd.

In order to apply (29) to the energy structure of a wire with $N_1=N_2=3$, we remember that for vanishing field the levels are given by

$$H_0'+|K_1|\begin{cases}0\\ \pm\sqrt{2}\end{cases}+|K_2|\begin{cases}0\\ \pm\sqrt{2}\end{cases}=0. \quad (30)$$

For $|K_1|=|K_2|$ we have a twofold degeneracy at $H_0'=\pm\sqrt{2}$ and a threefold degeneracy at $H_0'=0$. These degenerate levels are split in the magnetic field. Figure 4 shows the splitting owing to the bulk terms (24), which near $b=0$ yield a quadratic dependence on b. The dashed curves arise from solving $P(3,\frac{1}{4}\pi)=0$, the solid ones from solving $P(3,\frac{1}{2}\pi)=0$ and the dashed-dotted ones from solving $P(3,\frac{3}{4}\pi)=0$. In Fig. 5 the influence of the surface terms (29) is included. At $H_0'=\pm\sqrt{2}$ the level splitting is linear in b, whereas at $H_0'=0$ the repulsion is linear or quadratic. In both figures the curves were continued to larger values of b by a numerical

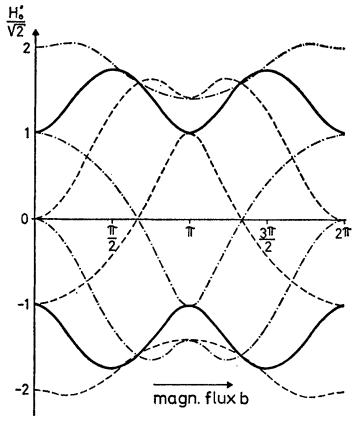

FIG. 4. Level splitting owing to the bulk terms for $N_1=N_2=3$.

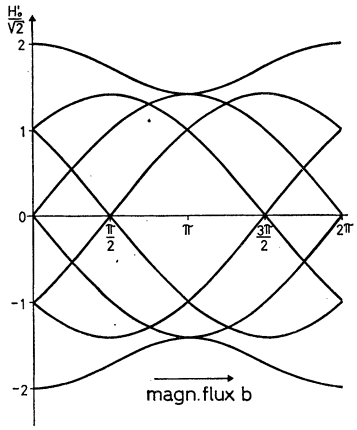

FIG. 5. Level splitting owing to the bulk and surface terms for $N_1=N_2=3$.

treatment. It is found that the bulk terms already yield a rather good approximation; the surface terms influence essentially the regions of degeneracy. The rule that the splitting is linear or quadratic according to the symmetry properties of the wave functions is also valid at $b=\pi$. The strong dependence of the levels on b as shown in Figs. 4 and 5 indicates the difficulties which are involved in extrapolations from strong to weak magnetic fields.

B. Energy Levels of Films

Films parallel and wires perpendicular to the magnetic field can be described by N_1 finite, N_2 infinite, and N_3 arbitrary. Thus, all surface terms vanish and the secular determinant reduces to the product of all bulk terms. In order to obtain the energy levels we transform these finite Peierls' determinants $P(N_1,\theta_2)$ and carry out a second-order perturbation calculation.

We perform the following sine transformation:

$$p(\theta_1',\theta_1)=\frac{2}{N_1+1}\sum_{\kappa',\kappa=1}^{N_1}\sin\kappa'\theta_1'\sin\kappa\theta_1 p_{\kappa',\kappa}, \qquad (31)$$

$$\theta_1=\mu_1\pi/(N_1+1);\quad \mu_1=1,\cdots,N_1.$$

This utilization of standing waves also in the a_1 direction proves reasonable; it is in analogy to (2) and (18), (19) and separates (24) for $b=0$. Summing over κ' and transforming the sum over κ yields

$$p(\theta_1',\theta_1)=[H_0'+2|K_1|\cos\theta_1+2|K_2|\cos\theta_2]\delta(\theta_1',\theta_1)$$
$$+\frac{2}{N_1+1}4|K_2|\sum_{\kappa=1}^{N_1}\sin\kappa\theta_1'\sin\kappa\theta_1\sin\tfrac{1}{4}(N_1-2\kappa+1)b\begin{cases}-\cos\theta_2\sin\frac{1}{4}(N_1-2\kappa+1)b\\ \sin\theta_2\cos\frac{1}{4}(N_1-2\kappa+1)b\end{cases}. \qquad (32)$$

The first term in (32) describes the well-known energy structure for vanishing field. The upper expression in the second term is valid for $\mu_1'+\mu_1$ even, the lower for $\mu_1'+\mu_1$ odd. We again have the result that the type of energy shift depends on the symmetry properties of the eigenfunctions. As the level system for vanishing field is not degenerate, we have a quadratic repulsion for eigenfunctions of different symmetry ($\mu_1'+\mu_1$ odd) and a fourth-power repulsion for equal symmetry ($\mu_1'+\mu_1$ even). To be exact up to the order b^2, we have to carry out a second-order perturbation treatment using wave functions of different symmetry. Summing over κ and inserting $\theta_1=\mu_1\pi/(N_1+1)$, Eq. (32) yields

$$p(\theta_1',\theta_1)=[H_0'+2|K_1|\cos\theta_1]\delta(\theta_1',\theta_1)+\frac{1}{N_1+1}|K_2|\frac{\sin\theta_1'\sin\theta_1\sin b}{\prod_{\pm,\pm}\sin[\theta_1'\pm\theta_1\pm b]/2}\begin{cases}-\cos\theta_2\sin(N_1+1)b/2\\ \sin\theta_2\cos(N_1+1)b/2\end{cases}. \qquad (33)$$

From Schrödinger's perturbation theory we obtain

$$H_0'+2|K_1|\cos\theta_1+2|K_2|\cos\theta_2\frac{\sin(N_1+1)b/2}{N_1+1}\cot\tfrac{1}{2}b\frac{\sin^2\theta_1}{\sin(\theta_1+\frac{1}{2}b)\sin(\theta_1-\frac{1}{2}b)}$$
$$-|K_1|\left(\frac{4}{N_1+1}\left|\frac{K_2}{K_1}\right|\sin\theta_2\sin b\right)^2\sum_{\substack{\mu_1'\\(\mu_1'+\mu_1\text{ odd})}}\frac{\sin^2\theta_1\sin^2\theta_1'\cos^2(N_1+1)b/2}{2(\cos\theta_1'-\cos\theta_1)(\cos(\theta_1'+b)-\cos\theta_1)^2(\cos(\theta_1'-b)-\cos\theta_1)^2}=0. \qquad (34)$$

Summation in (34) is feasible. We utilize the fact that the poles of the sum with respect to θ_1 are equidistant, calculate the corresponding residues, and obtain from the Mittag-Leffler theorem the energy expression

$$E=H_0+2|K_1|\cos\theta_1\left\{1-\left(b\left|\frac{K_2}{K_1}\right|\frac{\sin\theta_2}{\sin\theta_1}\right)^2\left[\frac{(N_1+1)^2+2}{24}-\frac{5}{8\sin^2\theta_1}\right]\right\}$$
$$+2|K_2|\cos\theta_2\left\{1-b^2\left[\frac{(N_1+1)^2+2}{24}-\frac{1}{4\sin^2\theta_1}\right]\right\}+2|K_3|\cos\theta_3, \quad (35)$$

$\theta_i=\mu_i\pi/(N_i+1)$, $\mu_i=1, 2, \cdots, N_i$; N_1 finite, N_2 infinite, and N_3 arbitrary. Equations (34) and (35) are valid on the condition that

$$\left|\frac{K_2}{K_1}\right|\frac{(N_1+1)b}{2\sin\theta_1}\ll 1. \quad (36)$$

This means that no closed orbits are allowed, and the electrons should move approximately on straight lines. Straight-line orbits are guaranteed if the field is weak (b small) or if the foil is thin (N_1 small). Curvature is also small if the electrons move very fast normal to the surfaces (velocity $2|K_1|\sin\theta_1$ large), or if the transition probability parallel to the surfaces is low ($|K_2|$ small).

Let us now discuss the energy levels following from (34) and (35). θ_2 is continuous and yields bands which are distinguished by the discrete parameter θ_1. The first-order perturbation term of (34) generates the correction term for $2|K_2|\cos\theta_2$ in (35). Owing to $\theta_1\geq\pi/(N_1+1)$, this bracket is always positive; it increases with θ_1 approaching $\frac{1}{2}\pi$. We obtain a narrowing of the bands formed by θ_2, where the exterior bands become broader than the interior ones. As this term leaves the level system unaltered at $\theta_2=\frac{1}{2}\pi, \frac{3}{2}\pi$, we find an enlarging of the level spacing at the edges of the complete level system and a concentration at the center.

The second-order perturbation term of (34) yields the correction term for $2|K_1|\cos\theta_1$. This bracket is negative for $\mu_1=1, N_1$, and otherwise positive. Thus, the extreme exterior bands are shifted outward, all the others are shifted inward. Again we obtain an enlarging of the spacing at the edges and a concentration in the center of the complete level system (see the solid lines in Fig. 6). The second-order perturbation term has no influence at $\theta_2=0, \pi$. The widths of the single θ_2 bands now remain unaltered except for the outermost.

Each of the perturbation terms discussed above has its θ_2 maximum at the zero of the other one. The energy shifts at $\theta_2=0, \frac{1}{2}\pi, \pi$ as shown in Fig. 7 for $N_1=11$, therefore, arise only from one of these terms. At the edges of the complete level system an equal level spacing is approached, which indicates equal-spaced Landau levels of infinite crystals.

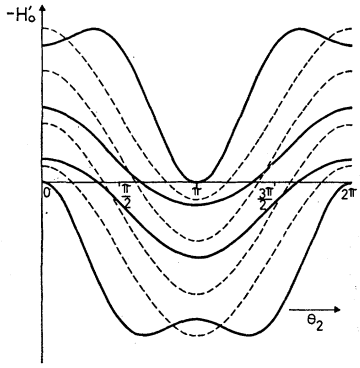

FIG. 6. The energy levels in foils according to the second-order perturbation treatment. Dashed curve: unperturbed. solid curve: perturbed.

C. Anisotropic Films in Strong Magnetic Fields

By calculating the influence of a weak magnetic field on the energy structure of films (see Fig. 6) we obtained a splitting which increases with increasing term density and indicates the mode of formation of Landau levels. For a deeper insight into this problem, and in order to calculate the level spacings explicitly, we assume in this section the crystal to be anisotropic with $|K_2|\gg|K_1|$, and thus can treat magnetic fluxes even of the order 1. Since interaction integrals depend exponentially on interatomic distances, this condition is satisfied even for small anisotropies. A most lucid but merely qualitative derivation of the level spacing for large fluxes is given in Sec. IIID.

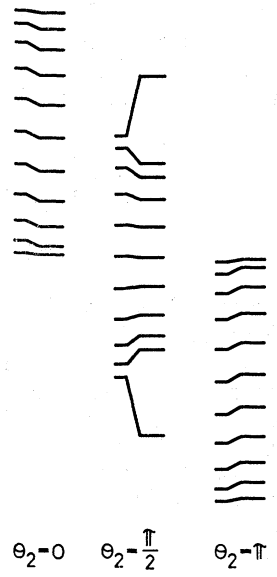

FIG. 7. The energy shift at $\theta_2=0$, $\pi/2$, π for $N_1=11$.

We again start from the finite Peierls' determinant (24) and solve it directly by a perturbation treatment. Thus, in contrast to the last section, we do not investigate standing waves in the a_1 direction but electrons localized in a single lattice plane. The first-order energy expressions are

$$H_0'+2|K_2|\cos(\theta_2-\kappa b)=0;$$
$$\kappa=-\tfrac{1}{2}(N_1-1),\ -\tfrac{1}{2}(N_1-3),\ \cdots,\ \tfrac{1}{2}(N_1-1). \quad (37)$$

Plotting H_0' versus θ_2 (see Fig. 8) we obtain energy curves which intersect at θ_2, $\pi-\theta_2=-\frac{1}{2}b(N_1-2)$, $-\frac{1}{2}b(N_1-3)$, $\cdots$, $\frac{1}{2}b(N_1-2)$. Interaction of these levels by the elements in the secondary diagonal of (24) yields an energy shift for all θ_2 and a splitting at the intersections. The shift of the state denoted by κ is mainly determined by the interaction with the states $\kappa\pm1$. We have to solve a subdeterminant of the order 3 and obtain

$$H_0'+2|K_2|\cos(\theta_2-\kappa b)$$
$$=\frac{|K_1|^2}{2|K_2|}\left(\frac{1}{\cos[\theta_2-(\kappa-1)b]-\cos[\theta_2-\kappa b]}\right.$$
$$\left.+\frac{1}{\cos[\theta_2-(\kappa+1)b]-\cos[\theta_2-\kappa b]}\right). \quad (38)$$

In (38) terms of the order $|K_1/K_2|^4$ are neglected because of the assumption $|K_2|\gg|K_1|$. Such terms arise from the interaction with the states $\kappa\pm2$, $\cdots$. However, these interactions are not negligible if we are interested in the splitting at the intersections. As the state κ_i interacts with the state κ_j by all states κ in between, we obtain the splitting of their intersections at θ_2, $\pi-\theta_2=\frac{1}{2}b(\kappa_i+\kappa_j)$ by investigating the subdeterminant built up from all elements belonging to $\kappa_i\leq\kappa\leq\kappa_j$.

Inserting the corresponding first-order energy expression $H_0'\pm2|K_2|\frac{1}{2}\cos\lambda b=0$, $\lambda=\kappa_j-\kappa_i$ into the principal diagonal for $\kappa_i<\kappa<\kappa_j$ yields a quadratic equation for the level splitting. By solving this equation we again obtain the shift (38) and, in addition, the gap width $\Delta H_0'$:

$$\frac{\Delta H_0'}{2|K_2|}=\frac{4|K_1/4K_2|^\lambda}{\sin^2\frac{1}{2}b\,\sin^2\frac{1}{2}2b\cdots\sin^2\frac{1}{2}(\lambda-1)b};$$
$$\lambda=1,\cdots,N_1-1. \quad (39)$$

From (39) we have the result that the splitting is large for small gap indices λ (near the edges of the complete level system); it decreases with increasing λ, i.e., when approaching the center of the level system. In Fig. 8 we plotted the unperturbed curves (37) and the levels shifted and split according to (38) and (39). The gap indicated by λ is extended over a θ_2 region of length $(N_1-\lambda)b$; it is still crossed by λ energy curves. As (38) does not depend explicitly on N_1, it is valid also for infinite crystals. The crossing of the gaps vanishes as soon as $N_1b>2\pi$ and the well-known Landau levels at the edges result. They are broadened when approaching the center of the level system and simultaneously the gaps are narrowed.

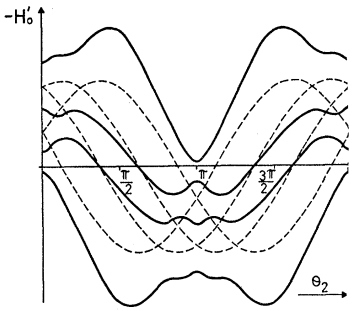

FIG. 8. Level spacing for electrons in single-lattice planes. Dashed curve: unperturbed; solid curve: perturbed.

As, in this section, we considered electrons chiefly located in a single-lattice plane, the gaps now appear as resonances for transitions between different planes. A process in which the electron is hopping to an adjacent plane yields a factor $|K_1/K_2|$. We have to assign to it the gap $\lambda=1$. Terms quadratic in $|K_1/K_2|$ arise from transitions between next-nearest-neighbor planes. This can be realized both by a virtual and by a real occupation of the plane in between. This yields the gap $\lambda=2$ and a quadratic contribution to the gap $\lambda=1$ which was neglected in (39) owing to the assumption $|K_2/K_2|\ll1$. Higher order processes can be interpreted in a similar way.

D. The Energy Structure of Infinite Crystals

In order to visualize the generation of the electron energy structure for both weak and strong fields and arbitrary values of $|K_1|$ and $|K_2|$, we treat (24) for $N_1\to\infty$ and magnetic fluxes $b=2\pi/M$, M integer. These values for the flux were introduced also by Harper,[13] Brailsford,[14] and Fischbeck[11] for obtaining appropriate boundary conditions. This choice of the flux is only a mild restriction. By the Floquet theorem (24) can be reduced to a finite determinant of the order M:

$$\begin{vmatrix} H_0'+2|K_2|\cos(\theta_2+b) & |K_1| & & |K_1|e^{-iM\phi} \\ |K_1| & H_0'+2|K_2|\cos(\theta_2+2b) & & \\ \vdots & & \ddots & \vdots \\ |K_1|e^{iM\phi} & & & H_0'+2|K_2|\cos(\theta_2+Mb) \end{vmatrix}$$
$$=0. \quad (40)$$

ϕ is the separation parameter following from Floquet's theorem; it can be reduced to the interval $0\leq\phi\leq2\pi/M$. The value of the determinant (40) is not changed if θ_2 is replaced by $\theta_2+2\pi/M$. The Fourier expansion of (40) thus contains only the term independent of θ_2 and ϕ, which is a polynomial $Q(M,h_0')$ of the order M in $h_0'=H_0'/(|K_1|^2+|K_2|^2)^{1/2}$, and the terms $\cos M\theta_2$, $\cos M\phi$. By introducing the parameter $\beta=|K_1K_2|/(|K_1|^2+|K_2|^2)$, which is especially adapted to the

symmetry of the crystal, we obtain

$$Q(M,h_0')=h_0'^M-h_0'^{M-2}\cdot M$$
$$+h_0'^{M-4}\left[\tfrac{1}{2}M(M-3)-\beta^2 M\left(1+2\cos\frac{2\pi}{M}\right)\right]-+\cdots$$
$$=2(-1)^M\beta^{M/2}\left[\left|\frac{K_1}{K_2}\right|^{M/2}\cos M\phi+\left|\frac{K_2}{K_1}\right|^{M/2}\cos M\theta_2\right]. \tag{41}$$

The solutions of (41) can be found by plotting $Q(M,h_0')$ versus h_0' and by looking for those values h_0' for which $Q(M,h_0')$ lies between the extremes of the right-hand side of (41), $\pm\beta^{M/2}[|K_1/K_2|^{M/2}+|K_2/K_1|^{M/2}]$. This is demonstrated for $|K_1|=|K_2|$ and $M=6$ in Fig. 9. We find six allowed energy zones; the exact zone boundaries are indicated. In general, the total number of allowed energy zones is equal to M, which implies that the number of zones and gaps increases with decreasing b. The amplitudes of $Q(M,h_0')$ increase with increasing $|h_0'|$; we obtain a broadening of the energy zones and a narrowing of the gaps when going from the edges to the center. Using the quasiclassical picture of closed and open electron orbits in θ space at the edges and at the center of the band, respectively, we find this broadening to be in agreement with the fact that the energies of closed orbits are more degenerate than those of open orbits. For b approaching zero the energy structure obviously becomes a continuum.

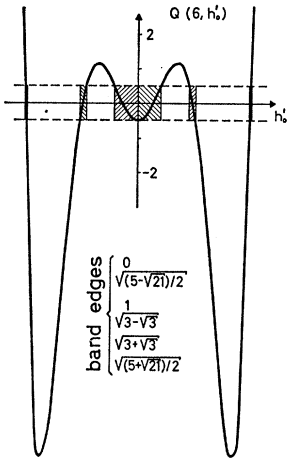

FIG. 9. Regions of allowed and forbidden energies for $b=2\pi/6$.

The zone boundaries can be calculated exactly from (41) for several values of M up to $M=8$. Thus the gap widths are also known explicitly. Comparison of the resulting expression with the gap width given in (39) shows an exact agreement for $|K_1|\ll|K_2|$ and also indicates that (39) can be extended to arbitrary values of $|K_1|$ and $|K_2|$ by introducing β, too. Instead of (39) this yields

$$\frac{\Delta H_0'}{(|K_1|^2+|K_2|^2)^{1/2}}=\frac{2\beta^\lambda}{4^{\lambda-1}\sin^2\tfrac{1}{2}b\sin^2\tfrac{1}{2}2b\cdots\sin^2\tfrac{1}{2}(\lambda-1)b};$$
$$\lambda=1,\cdots,M-1/2. \tag{42}$$

The maximum gap index λ is determined by the extension of the electron orbit. As in this section infinite crystals are considered, λ is given by the inverse magnetic field. For films the extension is either limited by the thickness $N_1|a_1|$ or in strong fields again by M. As long as the first limitation is valid, we still have a crossing of the gap λ by λ energy curves; this crossing ceases as soon as the gap is limited by the field.

Equation (42) is expected to approximate the gap width very closely at the center of the level system. This is due to the fact that the energy shift, which is large at the edges, was neglected when deriving the gap formula (39). It is found that the gap widths decrease exponentially when approaching the center, and that the innermost gap depends exponentially on the magnetic field according to $|K_1K_2/(|K_1|^2+|K_2|^2)|^{\pi/b}$. This is in agreement with qualitative conclusions of Harper.[14]

Equation (41) also allows an approximate determination of the energy-zone width (level broadening) at the edges. The slope of $Q(M,h_0')$ as resulting from its leading terms yields the inverse widths of the first zones (see Fig. 9). We find these widths to be proportional to $\exp(-\text{const}/b)$, which is in agreement with the level broadening as discussed by Brailsford.[15]